NEURAL REGENERATION RESEARCH
September 2014, Volume 9, Issue 17
www.nrronline.org

Autophagy occurs within an hour of adenosine triphosphate treatment after nerve cell damage: the neuroprotective effects of adenosine triphosphate against apoptosis

Na Lu[1], Baoying Wang[1], Xiaohui Deng[2], Honggang Zhao[1], Yong Wang[3], Dongliang Li[1]

1 Department of Physiology and Neurobiology, Xinxiang Medical University, Xinxiang, Henan Province, China
2 Department of Human Anatomy, Xinxiang Medical University, Xinxiang, Henan Province, China
3 Department of Laboratory Animal Center, Xinxiang Medical University, Xinxiang, Henan Province, China

Corresponding author:
Dongliang Li, Department of Physiology and Neurobiology, Xinxiang Medical University, Xinxiang 453003, Henan Province, China, xyldl8@126.com.

doi:*10.4103/1673-5374.141811*
http:*//www.nrronline.org/*

Accepted: *2014-08-17*

Abstract

After hypoxia, ischemia, or inflammatory injuries to the central nervous system, the damaged cells release a large amount of adenosine triphosphate, which may cause secondary neuronal death. Autophagy is a form of cell death that also has neuroprotective effects. Cell Counting Kit assay, monodansylcadaverine staining, flow cytometry, western blotting, and real-time PCR were used to determine the effects of exogenous adenosine triphosphate treatment at different concentrations (2, 4, 6, 8, 10 mmol/L) over time (1, 2, 3, and 6 hours) on the apoptosis and autophagy of SH-SY5Y cells. High concentrations of extracellular adenosine triphosphate induced autophagy and apoptosis of SH-SY5Y cells. The enhanced autophagy first appeared, and peaked at 1 hour after treatment with adenosine triphosphate. Cell apoptosis peaked at 3 hours, and persisted through 6 hours. With prolonged exposure to the adenosine triphosphate treatment, the fraction of apoptotic cells increased. These data suggest that the SH-SY5Y neural cells initiated autophagy against apoptosis within an hour of adenosine triphosphate treatment to protect themselves against injury.

Key Words: *nerve regeneration; neurons; adenosine triphosphate; SH-SY5Y cells; autophagy; apoptosis; cell culture; monodansylcadaverine; flow cytometry; cell viability; Bcl-2; Bax; Beclin 1; neuronal damage; NSFC grant; neural regeneration*

Funding: *This study was supported by the National Natural Science Foundation of China, No. 81371346, 81271376.*

Lu N, Wang BY, Deng XH, Zhao HG, WangY, Li DL. Autophagy occurs within an hour of adenosine triphosphate treatment after nerve cell damage: the neuroprotective effects of adenosine triphosphate ag ainst apoptosis. Neural Regen Res. 2014;9(17):1599-1605.

Introduction

Adenosine triphosphate is the most important molecule for energy storage *in vivo*. Adenosine triphosphate also plays an important role in the central nervous system. The role of adenosine triphosphate as a neurotransmitter in the nervous system was first reported in 1959 (Holton, 1959), and a diverse set of physiological actions by adenosine triphosphate have been revealed (Butt, 2011). Astrocytes release adenosine triphosphate to propagate an intercellular calcium wave (Cotrina et al., 1998; Guthrie et al., 1999), and the released adenosine triphosphate is also important in triggering cellular responses to trauma and ischemia (Burnstock, 2006; Franke et al., 2014). In addition, adenosine triphosphate stimulates astrocyte proliferation and contributes to the process of reactive astrogliosis (Ambrosini et al., 1994). Besides these functions, adenosine triphosphate is also involved in the regulation of neuronal excitability, initiation of pain, and mediation of intercellular communication (Cook et al., 1997; Avshalumov et al., 2005; Gomes et al., 2005). In the nervous system, adenosine triphosphate is an extracellular signaling molecule that is mainly released from exocytotic vesicles, and the concentration of nucleotides in such vesicles can reach 1,000 mmol/L. The released adenosine triphosphate is transported to the synaptic cleft, and selectively acts on receptors to perform its functions, which include neurotransmitter regulation, synaptic modification, and neurotrophy (Hernández, 1992; Froemke et al., 2006). Under normal physiological conditions, the concentration of extracellular adenosine triphosphate is relatively low (Illes et al., 2004; Köles et al., 2011). However, mechanical stress, hypoxia, inflammation, and certain agonists can lead to a massive release of adenosine triphosphate (Bodin et al., 2001). When the extracellular concentration of adenosine triphosphate reaches a certain level, secondary neuronal death occurs (Skaper et al., 2010). The main source of adenosine triphosphate acting on purinoceptors was reported

as deriving from damaged or dying cells (Burnstock, 2006). Therefore, research on the toxic effects of adenosine triphosphate on neurons may help to elucidate the process of neuronal death and provide new ideas for therapies targeting brain injury.

Human neuroblastoma cells SH-SY5Y were originally isolated from the neural crest during nervous development. They exhibit similar biochemical, pharmacological, and functional characteristics to neurons and are considered to be a good *in vitro* model for studying neuronal function, differentiation, and apoptosis. Autophagy, discovered after necrosis and apoptosis, is a third form of cell death. Prior research showed that autophagy has cerebral protective effects. When neurons are stressed, autophagy is first activated. When autophagy cannot maintain a steady state, cell apoptosis occurs, and finally necrosis. In the present study, SH-SY5Y cells were incubated in different concentrations of adenosine triphosphate for different lengths of time. After treatment, cell viability, autophagy, and apoptosis were measured. In addition, the expressions of Bcl-2, Bax, and Beclin 1 were also assessed. We hypothesized that autophagy removes and degrades damaged organelles to satisfy the metabolic demands of cells, as well as protect them (Zou et al., 2012).

Materials and Methods

Cell culture

SH-SY5Y cells were purchased from the Cell Bank, Chinese Academy of Sciences, Shanghai, China. The human neuroblastoma SH-SY5Y cell line was cultured in Dulbecco's modified Eagle's medium (DMEM; Gibco, Grand Island, NY, USA) supplemented with 10% fetal bovine serum (Hyclone, Logan, UT, USA) at 37°C with 5% CO_2. The medium was replaced every 48 hours. The cells were passaged until cell fusion occurred. Treatments were performed on cells in the logarithmic growth phase in this study.

Experimental groups

(1) Primary SH-SY5Y cell cultures were treated for 3 hours with one of six different concentrations of adenosine triphosphate as follows: DMEM control group; DMEM + adenosine triphosphate (Sigma, St Louis, MO, USA) at 2 mmol/L; DMEM + adenosine triphosphate at 4 mmol/L; DMEM + adenosine triphosphate at 6 mmol/L; DMEM + adenosine triphosphate at 8 mmol/L; or DMEM + adenosine triphosphate at 10 mmol/L.

(2) Primary SH-SY5Y cell cultures were treated with adenosine triphosphate at 6 mmol/L for different lengths of time as follows: DMEM control group (no adenosine triphosphate) or DMEM + adenosine triphosphate at 6 mmol/L for 1, 2, 3, or 6 hours.

Morphological examination

After treatment with different adenosine triphosphate concentrations (2, 4, 6, 8, or 10 mmol/L for 3 hours) and different exposure times (1, 2, 3, or 6 hours) of 6 mmol/L adenosine triphosphate, the morphology of the SH-SY5Y cells was observed with an inverted optical microscope.

Cell Counting Kit assay

SH-SY5Y cells were first thawed and seeded into 96-well plates at a density of 5×10^7 cells/well (100 μL). After being cultured in an incubator for 24 hours, the cell media were aspirated and replaced with new media containing different concentrations of adenosine triphosphate (2, 4, 6, 8, 10 mmol/L) for 3 hours. The serum-containing medium without adenosine triphosphate was used as a control ($n = 8$) (Wei et al., 2013).

The cell viability was assessed using a Cell Counting Kit-8 (CCK-8) kit (Guangzhou Jing Xin Biological Technology Co., Ltd., China), and the absorbance values were measured using a microplate reader at 570 nm. This experiment was performed in triplicate.

Cell viability was calculated as the $\text{absorbance}_{\text{adenosine triphosphate}}$ / $\text{absorbance}_{\text{control}} \times 100\%$, where absorbance is the mean value from five replicates, $\text{absorbance}_{\text{control}}$ is the control group absorbance, and $\text{absorbance}_{\text{adenosine triphosphate}}$ is the treatment group absorbance values.

Similarly, the effects of incubation time (1, 2, 3, or 6 hours) (Wei et al., 2013) at 6 mmol/L adenosine triphosphate on cell viability were also determined.

Monodansylcadaverine staining for autophagic vacuoles

Monodansylcadaverine staining was performed as previously described (Pamenter et al., 2012). Briefly, the cells were treated with 6 mmol/L of adenosine triphosphate for 1, 2, 3, or 6 hours. Then, 0.05 mmol/L monodansylcadaverine was added, and the cells were incubated at 37°C for another 60 minutes. After removing the monodansylcadaverine, the cells were fixed in 4% paraformaldehyde for 5 minutes at 4°C. Finally, the samples were observed using fluorescence microscopy (BX51 Olympus, Tokyo, Japan; excitation wavelength: 365 nm; blocking wavelength: 430 nm). Five randomly selected microscopic fields at 400 × magnification were used to quantify the fluorescence intensity with Image J software (National Institutes of Health, Bethesda, MD, USA), which represents the relative levels of cellular autophagy. The average fluorescence values were calculated from three biological replicates.

Detection of cell apoptosis

Flow cytometry (EPICS® ALTRA™; Olympus) was performed on cells treated with 6 mmol/L adenosine triphosphate for 1, 2, 3, or 6 hours. The cells were stained with propidium iodide at 1 μg/mL and Annexin V-FITC for 15 minutes at 37°C, and then the samples were washed twice with PBS. A minimum of 10,000 cells were collected for each sample, and the data were analyzed using FCS Express Flow Cytometry software (De Novo Software, Los Angeles, CA, USA). The flow cytometry software was used to directly calculate the percentage of apoptotic cells. The average % of apoptotic cells was calculated from three biological replicates.

Real-time PCR (RT-PCR)

RT-PCR was performed on cells after treatment with 6 mmol/L adenosine triphosphate for 1, 2, 3, or 6 hours. We performed the total RNA extraction using Trizol reagent (Invitrogen, Guangzhou, China). Reverse transcriptases (Life Technolo-

Table 1 Specific primers used in real time-PCR analysis

Gene	Primer sequence	Product size (bp)
Bcl-2	Forward: 5′-GGT GCC ACC TGT GGT CCA CCT G-3′	459
	Reverse: 5′-CTT CAC TTG TGG CCC AGA TAG G -3′	
Bax	Forward: 5′-GTT ACA GGG TTT CAT CCA GG-3′	550
	Reverse: 5′-CGT GTC CAC GTC AGC AAT -3′	
Beclin 1	Forward: 5′- ATC CTC GAC CGT GTC ACC ATC CAC-3′	365
	Reverse: 5′- GAT GAG CTG AGT GTC CAG CTG GG -3′	
β-Actin	Forward: 5′- ATC TGG CAC CAC ACC TTC TA-3′	242
	Reverse: 5′- CGT CAT ACT CCT GCT TGC TG-3′	

gies) were used to prepare complementary DNA according to the manufacturer's instructions. The expression levels were quantified on the ABIPR ISM 7500 system (Applied Biosystems, Foster City, CA, USA) using the SYBR Green I dye method (Toyobo, Shanghai, China). The expression levels of Bcl-2, Bax, and Beclin 1 were detected by PCR using the specific primers shown in **Table 1**. β-Actin was used as a control. The PCR program consisted of 95°C for 30 seconds, and then 40 cycles of 95°C for 5 seconds and 60°C for 34 seconds. The mRNA relative expression levels ($2^{-\triangle\triangle Ct}$) were calculated using a previous method (Li et al., 2013).

Western blot assay

Western blot assay was performed on the same samples used for RT-PCR analysis. The SH-SY5Y cells were separated into five groups (the same for groups in experimental groups (2)): (1) control group, (2) adenosine triphosphate incubation 1-hour group, (3) adenosine triphosphate incubation 2-hour group, (4) adenosine triphosphate incubation 3-hour group, and (5) adenosine triphosphate incubation 6-hour group. Western blot assay was performed using standard protocols. The cells were first lysed on ice with phenylmethyl sulfonyl-fluoride lysis buffer (Applygen Technologies Inc., Beijing, China) for 30 minutes. The lysed cells were collected by centrifugation at 12,000 × *g* for 5 minutes at 4°C to obtain the total protein, which was then quantified using the bicinchoninic acid protein assay (ShineGene, Shanghai, China). A total of 50 μg of protein was separated by sodium dodecyl sulfate polyacrylamide gel electrophoresis on 5–10% gels, and then transferred to nitrocellulose membranes. The membranes were blocked with 5% powdered skim milk in Tris-buffered saline with Tween (10 mmol/L Tris-HCl, pH 7.5, 150 mmol/L NaCl, 0.05% Tween-20) and incubated overnight with rabbit anti-human Bcl-2, rabbit anti-human Bax (1:1,000; Abcam, Cambridge, UK), rabbit anti-human Beclin 1 (1:1,000; Abgent Biotechnology, San Diego, CA, USA), or mouse anti-human GAPDH (1:3,000, Abgent Biotechnology) antibodies at 4°C. After washing, the membranes were incubated with horseradish peroxidase-conjugated IgG secondary antibodies (goat anti-rabbit and goat anti-mouse IgG/horseradish peroxidase; 1:1,000; KPL Biotechnology, Gaithersburg, MD, USA) for 1 hour at room temperature and visualized with an enhanced chemiluminescence reagent system (Pierce Biotechnology, Rockford, IL, USA). Grayscale densitometric scanning of the protein bands was performed with Quanti Scan software (National Institutes of Health) using GAPDH as the control. Data were expressed as the absorbance ratio of target protein to GAPDH.

Statistical analysis

Data were expressed as the mean ± SD, and analyzed using SPSS 11.0 software (SPSS, Chicago, IL, USA). One-sample Kolmogorov-Smirnov *Z* tests were used to determine whether the data were normally distributed before analysis. Comparisons between different groups were performed using one-way analysis of variance, and intragroup comparisons were performed using least significant difference tests. *P*-values less than 0.05 were considered statistically significant.

Results

Morphology of adenosine triphosphate-treated SH-SY5Y cells

After treatment with different concentrations of adenosine triphosphate for 3 hours or 6 mmol/L adenosine triphosphate for 1, 2, 3, or 6 hours, the morphology of the SH-SY5Y cells was significantly altered. As shown in **Figures 1** and **2**, most of the untreated SH-SY5Y cells were spindle-shaped, showing cell processes, strong adherence, and high contrast. In addition, a large number of particles were observed in the cytoplasm. After treatment, however, the cells became round and the numbers of adherent cells, cell processes, cell volume, and contrast were all decreased with increasing concentration of adenosine triphosphate and increased exposure to adenosine triphosphate. These changes indicated that the negative effects of adenosine triphosphate were concentration- and time-dependent.

Cell viability decreased after adenosine triphosphate treatment

Cell viability was determined to quantify the damaging effects of adenosine triphosphate on SH-SY5Y cells. After 3 hours of adenosine triphosphate treatment, the cell viabilities were significantly reduced to 81.7 ± 2.1% in 2 mmol/L, 64.2 ± 1.7% in 4 mmol/L, 50.5 ± 2.2% in 6 mmol/L, 30.6 ± 0.9% in 8 mmol/L, and 10.5 ± 0.7% in 10 mmol/L adenosine triphosphate ($P < 0.05$). These data further illustrate the concentration-dependent effects of adenosine triphosphate on SH-SY5Y cells. The effects of incubation time on cell viability were also analyzed, showing significant reductions in cell viability with time until 3 hours (1 hour: 55.4 ± 2.6%; 2 hours: 42.6 ± 1.3%; and 3 hours: 33.5 ± 0.7%) ($P < 0.05$). However, no difference was found between treatment for 3 and 6 hours (3 hours: 33.5 ± 0.7%; and 6 hours: 34.1 ± 2.5%).

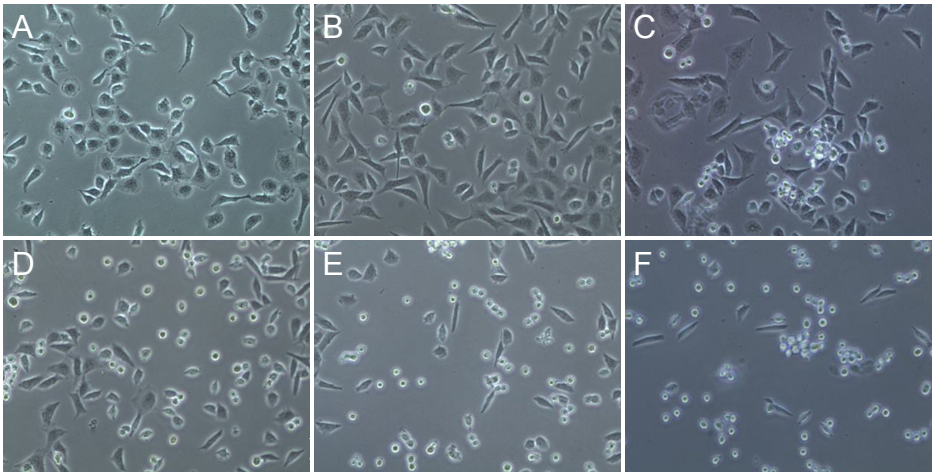

Untreated SH-SY5Y cells were spindle-shaped, showing cell processes, strong adherence, and good contrast (A). However, the cells became round after treatment, and the numbers of adherent cells, cell processes, cell volume, and contrast were all decreased with increasing concentration of adenosine triphosphate (B–F). (A) 0 mmol/L (DMEM control) group; (B–F) 2, 4, 6, 8, 10 mmol/L adenosine triphosphate groups, respectively.

Figure 1 Effects of adenosine triphosphate on the morphology of SH-SY5Y cells after treatment with different concentrations of adenosine triphosphate for 3 hours (inverted microscope, × 200).

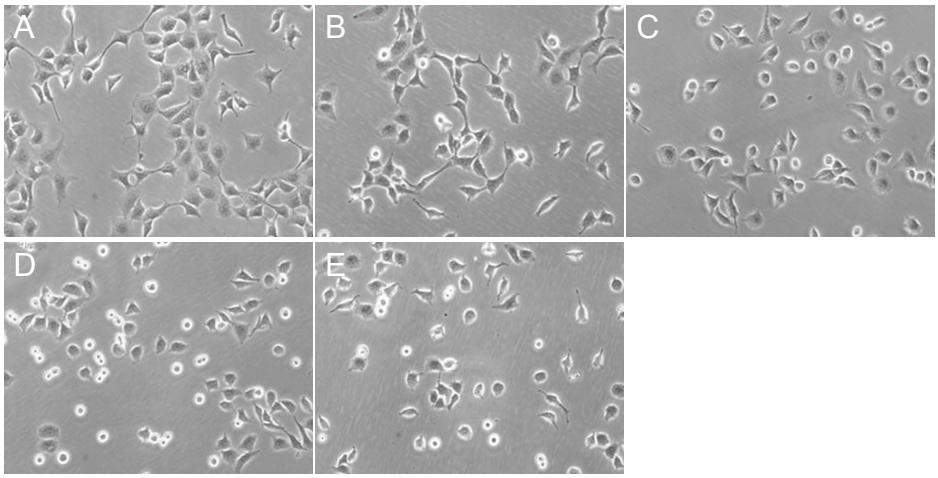

(A) Untreated SH-SY5Y cells were spindle-shaped, showing cell processes, strong adherence, and high contrast. (B–E) Cells became round after treatment. The numbers of adherent cells, cell processes, cell volume, and contrast were all decreased with increasing treatment times of 6 mmol/L adenosine triphosphate. (A) 0 hour (DMEM) group; (B–E) 1, 2, 3, and 6 hours of treatment groups, respectively.

Figure 2 Effects of adenosine triphosphate on the morphology of SH-SY5Y cells after treatment with 6 mmol/L adenosine triphosphate for 1, 2, 3, and 6 hours (× 200).

Adenosine triphosphate-induced formation of autophagic vacuoles

To observe the process of autophagy in SH-SY5Y cells after treatment with adenosine triphosphate, monodansylcadaverine staining was performed. The fluorescence intensity of the cells clearly reflected the relative levels of autophagic vacuoles. As shown in **Figure 3**, the fluorescence was significantly enhanced after 1 hour of treatment, as indicated by the appearance of a large number of autophagic vacuoles. However, the fluorescence began to decrease with prolonged treatment time.

Apoptosis increased after adenosine triphosphate treatment

After treatment with adenosine triphosphate, the apoptosis rates of the cells were detected using flow cytometry. As shown in **Figure 4**, the mean apoptotic population of normal SH-SY5Y cells was 2.11 ± 0.09%. However, the apoptotic fraction of treated cells was significantly increased in a time-dependent manner. The apoptosis rates were 6.23 ± 0.42% after 1 hour, 9.23 ± 0.21% after 2 hours, 11.60 ± 0.26% after 3 hours, and 30.51 ± 0.19% after 6 hours of treatment.

Adenosine triphosphate altered the expression of Bcl-2, Bax, and Beclin 1

Bcl-2 and Bax are both associated with apoptosis, and Beclin 1 is associated with autophagy. Therefore, we performed RT-PCR and western verification on adenosine triphosphate-treated cells to determine the expression levels of these genes. The expression of Bcl-2 was significantly reduced in treated groups compared with the control group, while the expression of Bax was significantly increased. Beclin 1 exhibited significantly increased levels after 1 hour of treatment. However, it began to decrease at prolonged treatment times (**Figure 5**).

Discussion

Apoptosis is an active cell death process. In this study, cell viability was significantly decreased in a concentration- and time-dependent manner by adenosine triphosphate treatment. In addition, the apoptosis rate was also significantly increased in a time-dependent manner. These results suggest that the adenosine triphosphate treatment initiated apoptosis in the cells. We also analyzed the expression of

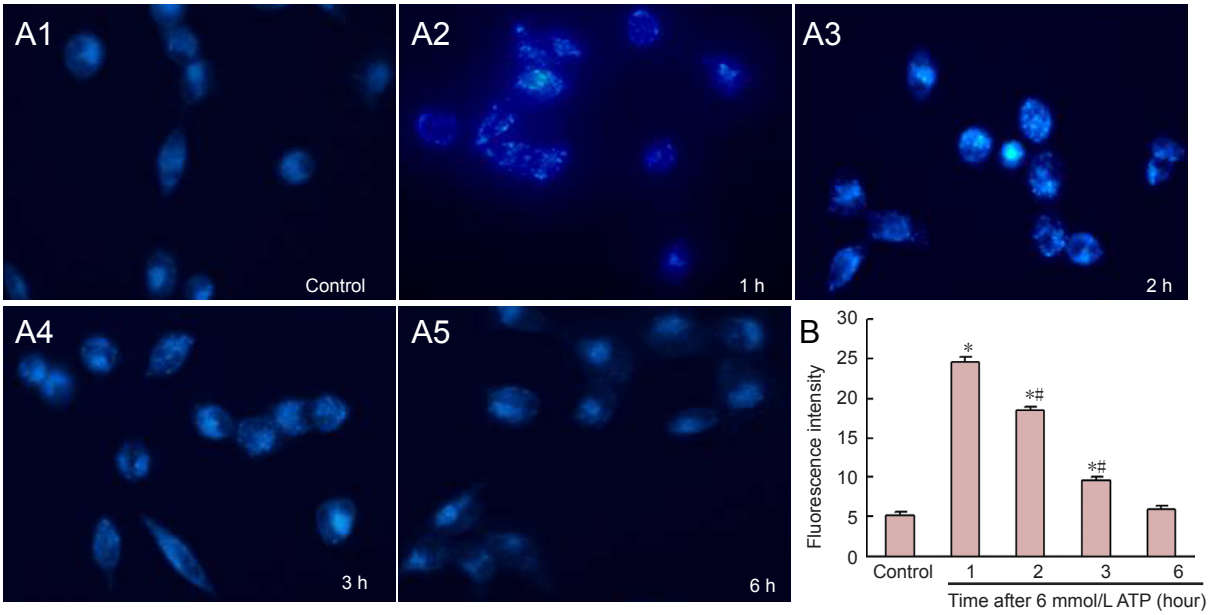

Figure 3 Autophagic vacuoles in SH-SY5Y cells exposed to 6 mmol/L adenosine triphosphate (ATP) (monodansylcadaverine staining, × 400).
(A1–A5) Monodansylcadaverine staining of autophagic vacuoles in SH-SY5Y cells after exposure to 6 mmol/L adenosine triphosphate for 1, 2, 3, and 6 hours. Strong monodansylcadaverine blue fluorescence signal in the cells identified autophagic vacuoles, and the fluorescence was significantly enhanced after an hour of treatment, which indicated the appearance of a large number of autophagic vacuoles. However, the fluorescence began to decline with prolonged treatment times. (B) The fluorescence intensity of monodansylcadaverine in SH-SY5Y cells after exposure to 6 mmol/L adenosine triphosphate for 1, 2, 3, and 6 hours. Data are expressed as the mean ± SD, $n = 3$. $*P < 0.05$ *vs.* the control group; $\#P < 0.05$, *vs.* the 1-hour group. Comparisons between different groups were performed using one-way analysis of variance, and intragroup comparisons were performed using the least significant difference tests. h: Hour.

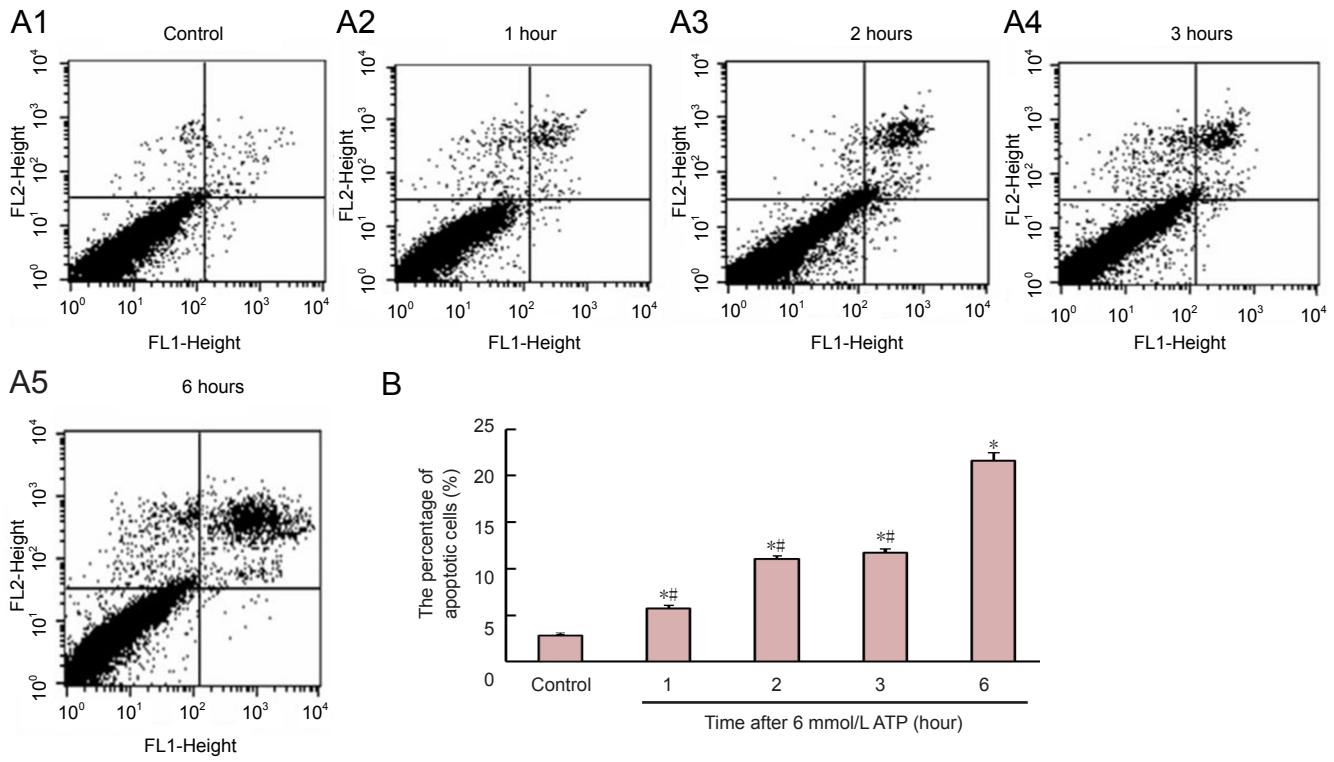

Figure 4 Flow cytometry detection of apoptosis in SH-SY5Y cell after treatment with 6 mmol/L adenosine triphosphate (ATP) for 1, 2, 3, and 6 hours.
(A) Flow cytometry of SH-SY5Ys cells incubated for 1, 2, 3, and 6 hours with 6 mmol/L ATP before double staining with annexin V-FITC and propidium iodide. The dotted plots show the annexin V-FITC on the x-axis and propidium iodide on the y-axis. Quadrants: Live cells (lower left); necrotic cells (upper left); apoptotic cells (upper right). (B) Compared with the controls, the percentage of apoptotic cells was significantly higher in the other groups after ATP treatment (mean ± SD, $n = 3$, $*P < 0.05$, *vs.* control group; $\#P < 0.05$ *vs.* the 6-hour group). Comparisons between the different groups were performed using one-way analysis of variance, and intragroup comparisons were performed using the least significant difference tests.

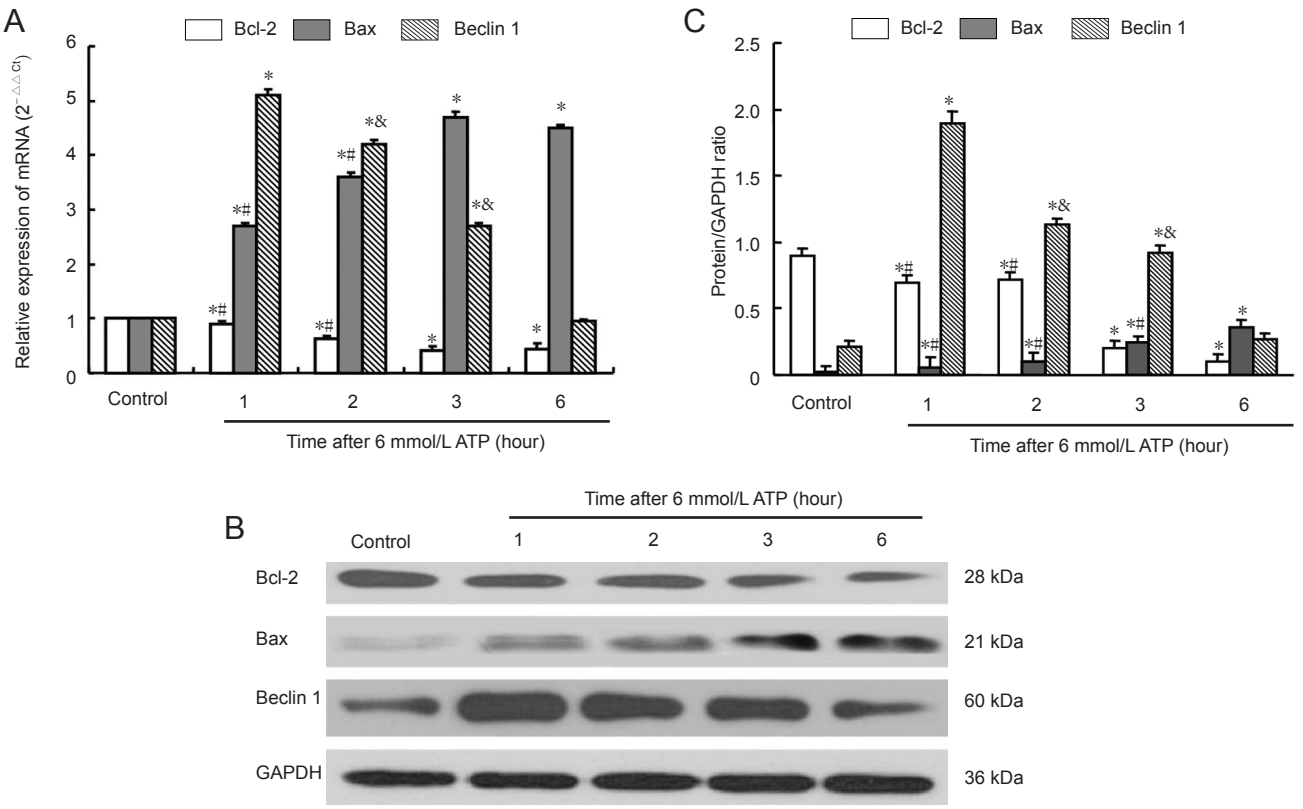

Figure 5 Effects of adenosine triphosphate (ATP) treatment time on the expression of Bcl-2, Bax, and Beclin 1 mRNA and protein in SH-SY5Y cells.

(A) Quantification of Bcl-2, Bax, and Beclin 1 mRNA expressions (RT-PCR). Data are expressed as absorbance of target protein to GAPDH. Compared with the untreated control group, Bax mRNA expression was significantly higher after treatment with 6 mmol/L ATP at all time points ($P < 0.05$). Bax mRNA expression peaked after 3 hours of treatment, while the Bcl-2 mRNA expression was significantly decreased ($P < 0.05$). Beclin 1 mRNA expression was significantly increased at 1, 2, and 3 hours ($P < 0.05$), showing the highest level after 1 hour and gradually decreasing with time. $*P < 0.05$, *vs.* control group; $\&P < 0.05$, *vs.* the 1-hour group; $\#P < 0.05$, *vs.* the 3-hour group. (B) Gel images from the western blots. (C) Quantification of Bcl-2, Bax, and Beclin 1 protein. Western blot assay showed that, compared with the untreated control group, Bax protein expression was significantly higher in all other groups after treatment with 6 mmol/L ATP ($P < 0.05$). Bax protein expression peaked at 6 hours, while the Bcl-2 expression was significantly decreased ($P < 0.05$). Beclin 1 protein expression was significantly increased at 1, 2, and 3 hours ($P < 0.05$), showing the highest level after 1 hour and gradually decreasing with time. $*P < 0.05$, *vs.* the control group; $\&P < 0.05$, *vs.* the 1-hour group; $\#P < 0.05$, *vs.* the 6-hour group. (A, C) Data were expressed as the mean ± SD. Comparisons between different groups were performed using one-way analysis of variance, and intragroup comparisons were performed the using least significant difference tests.

apoptosis-related proteins Bcl-2 and Bax. The expression of Bcl-2 was significantly decreased after adenosine triphosphate treatment, while the expression of Bax was increased. High expression levels of Bcl-2 and low Bax expression have been reported to induce high rates of apoptosis (Zhang, 2013). These phenomena further demonstrate the effects of adenosine triphosphate at high concentration on apoptosis.

Autophagy is a special form of cell death that is involved in the pathogenesis of brain injuries, neurodegenerative changes, and schizophrenia, among other diseases of the nervous system (Shpilka et al., 2011). Autophagy removes and degrades damaged organelles to satisfy the metabolic demands of cells, as well as protect them (Zou et al., 2012). Several external factors have been reported to induce autophagy such as starvation, hypoxia, high temperatures, and cellular stress (Feng et al., 2014). In the present study, we observed the process of autophagy in SH-SY5Y cells after treatment with adenosine triphosphate. We found that adenosine triphosphate significantly induced a large number of autophagic vacuoles after an hour of treatment. However, the number of autophagic vacuoles began to decline with prolonged treatment times. These changes indicate a positive role for autophagy during the repair of cell damage and these increases in autophagy occurred prior to the apoptosis peak at 6 hours. Further, we analyzed the expression of autophagy-related protein Beclin 1 and found a significantly increased expression level at 1 hour, which decreased over time. Beclin 1 is reported to be an upstream signaling molecule that can activate autophagy. Dissociated Beclin 1 forms a phosphatidylinositol 3-kinase III complex with a variety of proteins to participate in autophagy. In addition, upregulating the expression of Beclin 1 in mammalian cells may induce autophagy (Gabryel et al., 2012). Therefore, autophagy was likely initiated by the adenosine triphosphate treatment.

Based on our results, we suspect that adenosine triphosphate activates autophagy and apoptosis at the same time. When stress occurs in neurons, autophagy is first activated to protect neurons by maintaining neuronal homeostasis, to

reduce secondary injury, and to remove damaged organelles (Zeng et al., 2012; Zhao et al., 2012). However, excessive activation of autophagy may lead to apoptosis (Balduini et al., 2012; Pamenter et al., 2012). The accumulation of autophagic vacuoles appeared before apoptosis and was not affected by apoptosis inhibitors in prior studies. When autophagy was inhibited, the expression of Bcl-2 was also inhibited, though Bax was activated (Fayaz et al., 2014; Lin et al., 2014). Therefore, autophagy may lose its sensitivity to the adenosine triphosphate antagonist over time, leading to a decline in autophagy and acceleration of apoptosis (Lomonaco et al., 2011; Wang et al., 2012).

In summary, high concentrations of extracellular adenosine triphosphate first induced autophagy, and then led to apoptosis in SH-SY5Y cells. Further research on the regulation of autophagy and apoptosis mechanisms by the gliotransmitter adenosine triphosphate may lead to new ideas for the treatment and repair of neuronal injury.

Author contributions: *Li DL was in charge of funds, designed the study, provided technical support and revised the manuscript. Lu N was also in charge of funds, performed the experiments with Wang Y, and wrote the manuscript. Lu N, Deng XH, Zhao HG and Wang BY provided other technical support. All authors approved the final version of the paper.*
Conflicts of interest: *None declared.*

References

Ambrosini G, Di Iorio P, Ballerini P, Ambrosini G, Giuliani P, Tiboni GM, Caciagli F (1994) Effects of exogenous ATP and related analogues on the proliferation rate of dissociated primary cultures of rat astrocytes. J Neurosci Res 39:556-566.

Avshalumov MV, Chen BT, Koós T, Tepper JM, Rice ME (2005) Endogenous hydrogen peroxide regulates the excitability of midbrain dopamine neurons via ATP-sensitive potassium channels. J Neurosci 25:4222-4231.

Balduini W, Carloni S, Buonocore G (2012) Buonocore, autophagy in hypoxia-ischemia induced brain injury. J Matern Fetal Neonatal Med 25:30-34.

Bodin P, Burnstock G (2001) Purinergic signalling: ATP release. Neurochem Res 26:959-969.

Burnstock, G (2006) Historical review: ATP as a neurotransmitter. Trends Pharmacol Sci 27:166-176.

Butt AM (2011) ATP: a ubiquitous gliotransmitter integrating neuron–glial networks. Semin Cell Dev Biol 22:205-213.

Cook SP, Vulchanova L, Hargreaves KM, Elde R , McCleskey EW (1997) Distinct ATP receptors on pain-sensing and stretch-sensing neurons. Nature 387:505-508.

Cotrina ML, Lin JH, Nedergaard M (1998) Cytoskeletal assembly and ATP release regulate astrocytic calcium signaling. J Neurosci 18:8794-8804.

Fayaz SM, Suvanish Kumar VS, Rajanikant GK (2014) Necroptosis: who knew there were so many interesting ways to die? CNS Neurol Disord Drug Targets 13:42-51.

Feng Y, He D, Yao Z, Klionsky DJ (2014) The machinery of macroautophagy. Cell Res 24:24-41.

Franke H, Illes P(2014) Nucleotide signaling in astrogliosis. Neurosci Lett 17:14-22.

Froemke RC, Tsay IA, Raad M, Long JD, Dan Y (2006) Contribution of individual spikes in burst-induced long-term synaptic modification. J Neurophysiol 95:1620-1629.

Gabryel B, Kost A, Kasprowska D (2012) Review-Neuronal autophagy in cerebral ischemia–a potential target for neuroprotective strategies? Pharmacol Rep 64:1-15.

Gomes P, Srinivas SP, Vereecke J, Himpens B (2005) ATP-dependent paracrine intercellular communication in cultured bovine corneal endothelial cells. Invest Ophth Vis Sci 46:104-113.

Guthrie PB, Knappenberger J, Segal M, Bennett MV (1999) ATP released from astrocytes mediates glial calcium waves. J Neurosci 19:520-528.

Hernández RJ (1992) Na+/K (+)-ATPase regulation by neurotransmitters. Neurochem Int 20:1-10.

Holton P (1959) The liberation of adenosine triphosphate on antidromic stimulation of sensory nerves. J Neurophysiol 145:494-504.

Illes, P, Alexandre Ribeiro J (2004) Molecular physiology of P2 receptors in the central nervous system. Eur J Pharmacol 483: 5-17.

Köles L, Leichsenring A, Rubini P, Illes P (2011) P2 receptor signaling in neurons and glial cells of the central nervous system. Adv Pharmacol 1:441-493.

Li F, Li L, Zhong Y, Xie Q, Huang J, Kang X, Wang D, Xu L, Huang T (2013) Relationship between LTR methylation and gag expression of HIV-1 in human spermatozoa and sperm-derived embryos. PLoS One 8:e54801.

Lin Y, Cai B, Xue XH, Fang L, Wu ZY, Wang N (2014) TAT-mediated delivery of neuroglobin attenuates apoptosis induced by oxygen-glucose deprivation via the Jak2/Stat3 pathway in vitro. Neurol Res [Epub ahead of print].

Lomonaco SL, Finniss S, Xiang C, Lee HK, Jiang W, Lemke N, Rempel SA, Mikkelsen T, Brodie C (2011) Cilengitide induces autophagy-mediated cell death in glioma cells. Neuro Oncol 13:857-865.

Pamenter ME, Perkins GA, McGinness AK, Gu XQ, Ellisman MH, Haddad GG (2012) Autophagy and apoptosis are differentially induced in neurons and astrocytes treated with an in vitro mimic of the ischemic penumbra. PLoS One 7:e51469.

Shpilka T, Elazar Z (2011) Shedding light on mammalian microautophagy. Dev Cell 20:1-2.

Skaper SD, Debetto P, Giusti P (2010)The P2X7 purinergic receptor: from physiology to neurological disorders. FASEB J 24:337-345.

Wang P, Guan YF, Du H, Zhai QW, Su DF, Miao CY (2012) Induction of autophagy contributes to the neuroprotection of nicotinamide phosphoribosyltransferase in cerebral ischemic stroke. Autophagy 8:77-87.

Wei Q, Zhang Y, Jia X, Huai W, Yu C, Wan Z, Han L (2013) High dose of extracellular ATP switched autophagy to apoptosis in anchorage-dependent and anchorage-independent hepatoma cells. Purinerg Signal 9:585-598.

Zeng R, He J, Peng J, Chen Y, Yi S, Zhao F, Cui G (2012) The time-dependent autophagy protects against apoptosis with possible involvement of Sirt1 protein in multiple myeloma under nutrient depletion. Ann Hematol 91:407-417.

Zhang T, Saghatelian A (2013) Emerging roles of lipids in BCL-2 family-regulated apoptosis. Biochim Biophys Acta 1831:1542-1554.

Zhao Y, Chen G, Zhang W, Xu N , Zhu JY, Jia J, Sun ZJ, Wang YN, Zhao YF (2012) Autophagy regulates hypoxia-induced osteoclastogenesis through the HIF-1α/BNIP3 signaling pathway. J Cell Physiol 227:639-648.

Zou W, Wang X, Vale RD, Ou G (2012) Autophagy genes promote apoptotic cell corpse clearance. Autophagy 8:1267-1268.

Copyedited by McCarty W, Frenchman B, Wang J, Qiu Y, Li CH, Song LP, Zhao M